



INTERNATIONAL ATOMIC ENERGY AGENCY
UNITED NATIONS EDUCATIONAL, SCIENTIFIC AND CULTURAL ORGANIZATION
INTERNATIONAL CENTRE FOR THEORETICAL PHYSICS
I.C.T.P., P.O. BOX 586, 34100 TRIESTE, ITALY, CABLE: CENTRATOM TRIESTE



SMR/382- 23

WORKSHOP ON SPACE PHYSICS:
"Materials in Microgravity"
27 February - 17 March 1989

"Capillarity and Materials Properties" - I

A. PASSERONE
CNR
Istituto di Chimica Fisica Applicata dei Materiali
Genova, Italy

Please note: These are preliminary notes intended for internal distribution only.

WORKSHOP ON
SPACE PHYSICS: MATERIALS IN MICROGRAVITY

27 February-17 March 1989
TRIESTE

International Centre for Theoretical Physics

CAPILLARITY AND MATERIALS PROPERTIES

Alberto Passerone

Istituto di Chimica Fisica Applicata dei Materiali del CNR
Lungobisagno Istria 34, 16141, Genova, Italy.

INTRODUCTION

Microgravity represents an unprecedented tool to verify natural laws, as found in physics, chemistry, biology and so on, under conditions that can not be obtained in our 'classical' laboratories.

Certainly, general laws are able to take into account the presence, or not, of 'weight' so that no revolution will come from experiments in Space. However, physical and chemical processes are very often interpreted on the basis of theoretical models which, for the sake of clarity, take into account only a certain number of 'mechanisms', leaving out other possible contributions, considered as negligible.

When experimenting in space the same approximations cannot be made longer: neglected mechanisms may become predominant and the whole process may reveal new properties which may result in products with unexpected characteristics.

It is obvious that liquid phases are affected by the microgravity conditions: hydrostatics, hydrodynamics, phase separation, chemical reactivity have all to be reconsidered, if processes involving these disciplines are to be performed in Space.

When free surfaces or interfaces between different (fluid) phases are present, capillary phenomena develop, giving rise to particular shapes of the surfaces under study, and to special movements on them. These effects are always present, on Earth and in Space; however, on Earth, weight forces tend to conceal them, especially if large volumes are involved.

In Space, on the contrary, capillarity may become the main driving force, or physical quantity, characterizing many technological processes.

We shall review in the following, the basic principles which govern capillarity, with a special emphasis on the thermodynamic approach. Then, the main capillary phenomena, which are of a particular interest in μ -gravity will be examined, and a selected number of experiments already performed in various flights in the field of Materials Science, will be presented.

Then, problems related to specific surfaces and interfaces will be examined, either to present some particular effects arising in μ -gravity and affecting the material processing, or to discuss new developments in the physical-chemistry of surfaces.

The principal methods to measure surface properties will also be presented, paying a special attention to their possible application in a μ -gravity environment.

A. PRINCIPLES OF CAPILLARITY.

1. The surface tension.

Two fluids, for example one liquid and one gas phase or two liquid phases, are in general separated by a thin layer, which we call INTERFACE, whose properties are different from those of the two bulk phases.

This system behaves as it were formed by two fluid, homogeneous phases separated by an elastic membrane of infinitesimal thickness, under a state of uniform stress. This mechanical analogy, firstly proposed by Young in 1805, suffers from many limitations and can not be applied to multicomponent systems; it is however useful to introduce the concept of SURFACE TENSION σ .

Let us consider a geometrical surface, coinciding with the interface between the two phases, and let us trace on it an imaginary line AB, dividing in two parts the interface itself. If region 2 exerts a force σdl in the point P in a direction tangent to the surface in the same point, then σ is called the "surface tension" (or interfacial tension) in the point P.

The surface is in a state of uniform tension if:

a) σ is perpendicular to the dividing line AB in all points, and has the same value regardless of the orientation of the line AB.

b) σ has the same value in all the points of the surface.

Thus, the surface tension has the dimensions of a force on a unit length, and is usually measured in N/m (or mN/m).

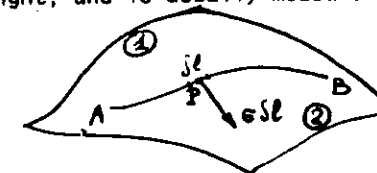


Fig.1

2) Junction among three phases.

If three phases, immiscible each other, meet, a special line where the three-phase contact takes place can be singled out. In each point of this line the three interfacial tensions $\sigma_{12}, \sigma_{13}, \sigma_{23}$ must be in mechanical equilibrium, that is

$$\sigma_{12} + \sigma_{13} + \sigma_{23} = 0$$

1.

A particular, but extremely interesting case, is represented by a system formed by a solid material in contact with two fluid phases. If the solid surface is planar, equation 1 then takes on the familiar form of the Young equation

$$\sigma_{23} = \sigma_{13} + \sigma_{12} \cos \theta$$

2.

which is largely used when dealing with problems concerning wettability, sintering, welding etc.

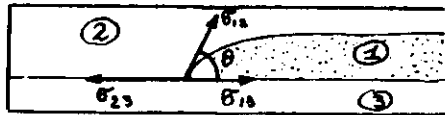


Fig.2.

3) Work of adhesion.

Consider now a system formed by a solid phase in contact with a liquid one, with a unit contact area.

We define "reversible work of separation" the free energy difference between the status 1 and 2 shown in fig.3.

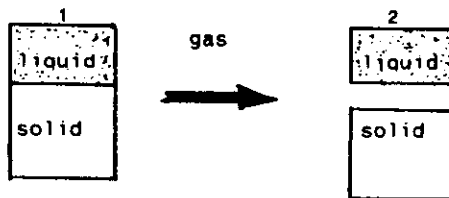


Fig.3

When passing from the configuration 1 to the configuration 2 a solid-liquid interface disappears and two new surfaces appear, namely: one liquid-vapour and one solid-vapour interface. The reversible work of adhesion is then

$$W = \sigma_{1g} + \sigma_{2g} - \sigma_{12}$$

3

If we apply eq.3 to a system formed by a planar solid material in contact with two fluid phases, we obtain, from eqs.2 and 3:

$$W = \sigma_{1g} (1 + \cos \theta)$$

4

The thermodynamic work of adhesion can then be computed if the liquid-vapour interfacial tension and the contact angle are known, for example, from an experiment involving the sessile-drop technique.

d) Surface thermodynamics. Adsorption.

Let us consider again two homogeneous fluid phases separated by an interface: this one has, in general, a certain thickness

and a composition different from that of the two contiguous phases.

In order to define the system thermodynamically, it is useful to employ the Gibbs model: the two phases are considered homogeneous and at constant composition up to an ideal dividing surface, to whom all the properties of the real interfacial phase are attributed (Fig.4).

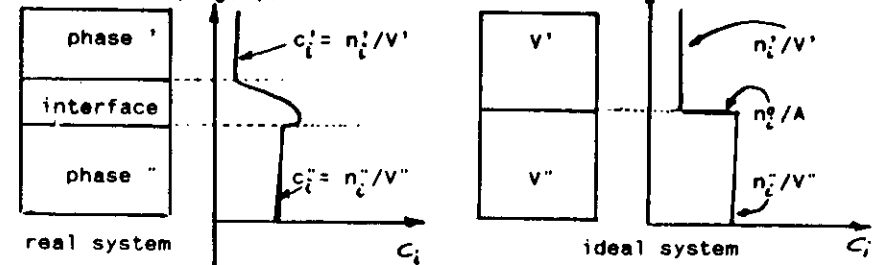


Fig.4.

If we call c_i' the concentration of component i in the volume V' , then $n_i' = c_i' V'$ and, similarly, $n_i'' = c_i'' V''$. If the system contains a total number n_i of moles of i , then

$$n_i = n_i' + n_i'' + n_i^s$$

5.

The number of moles adsorbed on the surface, also called "surface excess", is

$$n_i^s = n_i - n_i' - n_i''$$

6.

It is interesting to note that n^s can be either positive or negative (or zero).

We call "adsorption of i " at the surface, the quantity

$$\Gamma_i = n_i^s / A$$

7.

This quantity varies by varying the position of the dividing surface, as can be easily seen by writing

$$\Gamma_i = 1/A (n_i - c_i' V' - c_i'' V'')$$

In order to overcome this difficulty, the concept of "relative adsorption" has been introduced, defined as

$$\Gamma_{i,1} = \Gamma_i - \Gamma_1 \frac{c_i' - c_i''}{c_1' - c_1''} = \frac{1}{A} \left[(n_i - c_i' V') - \left(n_1 - c_1' V' \right) \frac{c_i' - c_i''}{c_1' - c_1''} \right]$$

8.

This new quantity does not depend on the position of the dividing surface, as seen in eq. 8.

In particular, if the phase $'$ is a gas, we can write, more easily

$$\Gamma_{i,1} = \Gamma_i - \Gamma_1 \frac{X_i}{X_1}$$

9.

Eq.9 is particularly useful when dealing with liquid metallic alloys.

e) Surface free energy.

From the first and the second principle of thermodynamics applied to a capillary system we have:

$$dQ = dU + p'dV' + p''dV'' - \sigma dA \quad 10.$$

$$dS = dQ/T + dQ^{irr}/T \quad 11.$$

$$\text{where } dQ^{irr} = -\sum \mu_i' dn_i' - \sum \mu_i'' dn_i'' - \sum \mu_i^s dn_i^s \quad 12.$$

so that

$$dF = -SdT - p'dV' - p''dV'' + \sigma dA + \sum \mu_i' dn_i' + \sum \mu_i'' dn_i'' + \sum \mu_i^s dn_i^s \quad 13.$$

where F represents the Helmholtz free energy.

Let us consider now a capillary system at constant T and V. F^s , the surface free energy, is then a function of (A, $n_1^s, n_2^s, \dots, n_i^s$), so that we can write

$$F^s = A \frac{dF^s}{dA} + \sum n_i^s \frac{dF^s}{dn_i^s} \quad 14.$$

Dividing by the total interfacial area A, we get

$$\frac{F^s}{A} = \frac{\partial F^s}{\partial A} + \sum_i \frac{n_i^s}{A} \frac{\partial F^s}{\partial n_i^s} \quad 15.$$

or

$$f^s = \sigma + \sum_i \Gamma_i \mu_i \quad 16.$$

because, from eq. 13, at T, V and number of moles constant, $dF/dA = \sigma$.

Equation 16 clearly shows that, in general, the interfacial tension σ can not be identified with the free surface energy per unit area f^s .

(However, this is true for a pure liquid, where the "chemical" terms vanish).

From eq.16 it is then possible to write

$$d\sigma = -s^s dT - \sum_i \Gamma_i d\mu_i \quad 17.$$

where s^s represents the surface entropy (excess quantity) per unit area.

Equation 17 is most useful when studying multicomponent systems, and is called the GIBBS ADSORPTION LAW.

B) LIQUID-VAPOUR INTERFACES

In multicomponent liquid systems, the distribution of various components is, in general, different near the surface with respect to the volume.

Adsorption of the i th component is greater the larger the decrease in surface free energy when its concentration increases in the bulk liquid phase.

In order to describe the surface behaviour of solutions, thermodynamic models are used, which are based on particular hypotheses on the structure of the system, on the type of bonding between atoms and so on.

The simplest model, or model of perfect surface solutions, is formally analogous to the model of bulk ideal solutions.

In this model we assume that the different phases in reciprocal contact through their interfaces, are represented by ideal solutions and that the interfaces could be represented by a monolayer. All atoms have the same size and the different species are assumed to be randomly distributed. This model leads to the following expression:

$$\sigma = \sigma_i + RT/\Omega \ln \frac{X_i^s}{X_i} \quad 1-8$$

where σ represents the interfacial tension of component i in its pure state, X_i^s its molar fraction on the monolayer, X_i its molar fraction in the bulk and Ω the total molar area.

This model is valid in a limited number of cases, especially in metallic systems like Ag-Cu, Cu-Ni, Au-Bi, Ge-Bi and few others.

However, in the great majority of cases, real systems do not follow this simple model.

Models based on statistical thermodynamics, are much more useful when dealing with metal-gas systems. This treatment still retains the hypothesis of interface one monolayer thick: indeed, recent Auger studies have confirmed that the segregation of "gaseous" solutes like oxygen, sulphur etc. is limited to one or two layers.

The Langmuir model, one of the best known, assumes that the surface is composed by a well defined number of sites, that can be occupied by the segregating atoms, and that between the adsorbed atoms no interactions exist.

The complete treatment leads to the relationship

$$\sigma = \sigma_1 + RT \Gamma_{2,1} \ln(1 - \theta) \quad 2-8$$

where θ represents the fraction of the occupied sites on the surface (surface coverage $0 \leq \theta \leq 1$)

$\Gamma_{2,1}$ represents the value of the maximum relative adsorption.

However, the Langmuir model, which forecasts that $X_2 = X_1^s$ for $\Gamma_{2,1} = 1/2$ (see fig. 5), is not in accord with the great majority of experimental observations, where the adsorption curve results steeper.

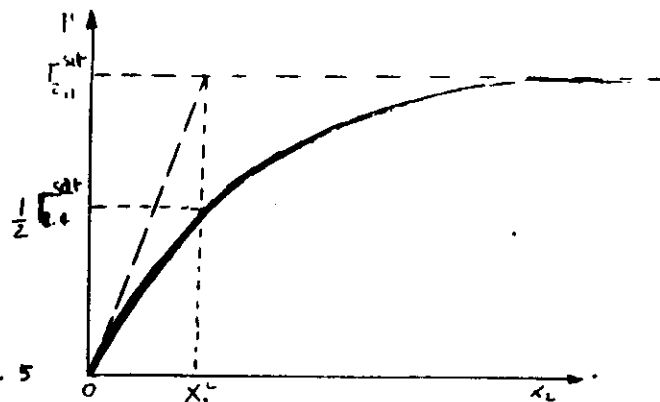


Fig. 5

In order to follow better the experimental behaviour, it is necessary to take into account other parameters, and, first of all, the interaction energy between adsorbed atoms.

We have recently presented a model, leading to an adsorption isotherm which allows, in the specific case of metal-oxygen systems, to interpret, correctly, the experimental variation of the surface tension of a liquid metal as a function of its oxygen content.

This model, which is a development of the classical Fowler-Guggenheim approach, is based, schematically, on the following hypotheses:

- i) Interface one monolayer thick,
- ii) Only nearest-neighbours interactions,
- iii) Metal-metal interaction parameters evaluated from the vaporization enthalpies,
- iv) Metal-oxygen interaction parameters evaluated from the dissolution enthalpy of component 2 (oxygen) into the liquid metal,
- v) The relative adsorption $\Gamma_{2,1}$ is set equal to Γ_2 , in view of the small concentration of component 2 in the bulk liquid,
- vi) A parameter is introduced: "f", which takes into account the stoichiometry of possible surface compounds. Its role is to act as an "exclusion rule".

The treatment starts considering the formal adsorption reaction



Here, O_{bulk} represents the oxygen dissolved in the liquid metal, V_{surf} the number of surface sites that oxygen can occupy, and O_{surf} the oxygen atoms in the surface monolayer.

The equilibrium constant of reaction 3-B, in the case the adsorbed atoms interact each other, can be written

$$K = \frac{\Gamma_2}{a_2(M-f\Gamma_2)} \exp\left(-\frac{\Delta E}{RT}\right) \quad 4-B$$

where

- a_2 = activity of oxygen in the bulk liquid,
- Γ_2 = surface adsorption of oxygen, which is nearly equal to its surface concentration,
- M = number of oxygen moles per unit area in a compact oxygen

monolayer,

$$\Delta E = E_{v1} - E_{surf}$$

The factor f takes into account that not all the surface sites can be occupied by oxygen atoms. Indeed, if the formation of compounds of the type Me_nO_m is allowed for in the surface monolayer, it is then necessary to take into account that each oxygen atom occupies $f = (n+m)/m$ sites. The more usual cases correspond to the formation of the following oxides: Me_2O ($f=3$); MeO ($f=2$); Me_2O_3 ($f=1.67$); MeO_2 ($f=1.5$).

By defining with $\epsilon_{11}, \epsilon_{22}$ and ϵ_{12} the interaction pair potentials between two metallic atoms, two oxygen atoms and one metal atom with one oxygen atom respectively, we get

$$\Delta E = \frac{1}{2} Z m \epsilon_{12} + \frac{1}{2} Z l f \theta (\epsilon_{12} - \epsilon_{22}) \quad 5-B$$

where Z is the total coordination number,
 l is the fraction of nearest neighbours in a plane parallel to the surface,
 m is the fraction of nearest neighbours in an adjacent plane; it is $2m + l = 1$.

If we define

$$\begin{aligned} \frac{1}{2} Z \epsilon_{11} &= -H_{vap} \\ \frac{1}{2} Z \epsilon_{12} - \frac{1}{2} Z \epsilon_{11} &= H_{diss} \end{aligned}$$

we get

$$E = a f \theta + b \quad 6-B$$

with

$$\begin{aligned} a &= (H_{diss} - H_{vap} - \frac{1}{2} Z \epsilon_{22}) \\ b &= m (H_{diss} - H_{vap}) \end{aligned}$$

The final expression of the surface tension then becomes

$$\sigma = \sigma^* + RT M \left\{ \frac{a f \theta^2}{2 RT} + \frac{1}{f} \ln(1-f\theta) \right\} \quad 7-B$$

It is possible to show that the energetic term a is subject to the conditions

$$a \leq \frac{RT}{f\theta(1-f\theta)} = 4 RT \text{ (maximum value)} \quad 8-B$$

If $a > 4 RT$, the surface should undergo a phase transition; a two phase region should exist between the two θ values defined as

$$\frac{1}{2f} \left(1 - \sqrt{1 - \frac{4aR}{a}} \right) \leq \theta \leq \frac{1}{2f} \left(1 + \sqrt{1 - \frac{4aR}{a}} \right) \quad 9-B$$

It is possible, from eqs. 4-B and 7-B, by suitably fitting experimental data of σ as a function of bulk concentration, to calculate the values of a for the particular system under study, and then to obtain an estimation of the parameter ϵ_{22} .

It is of a particular interest to examine the results obtained on different Me-O systems obtained by different authors (table 1).

metal	α (kJ/mol)	$-\frac{1}{2}\epsilon_{22}$ (kJ/mol)
Ag	23	319
Co	3	502
Cu	57	497
Fe	21	497
Ni	36	526

Table 1

We note here that the dissociation energy of the oxygen molecule ($O_2 \rightarrow 2O$) is 493.6 kJ/mol !

Moreover, the model proposed is able to treat systems with an oxygen concentration ranging from the value corresponding to the maximum adsorption (X_{max}), to the bulk saturation concentration (X_{sat}).

The rigorous relationship reads

$$\ln \left[X_{\text{sat}} \left(1 - X_{\text{ex}} \right)^{\frac{1 - X_{\text{sat}}}{X_{\text{sat}}}} \right] = \ln \left[X_{\text{ex}} \left(1 - X_{\text{sat}} \right)^{\frac{1 - X_{\text{sat}}}{X_{\text{sat}}}} \right] + \frac{G_{\text{ox}} - G_{\text{sat}}}{P_{\text{max}} RT} \quad 10-B$$

Fig. 6 shows that this relationship is verified by all experimental systems investigated up to now.

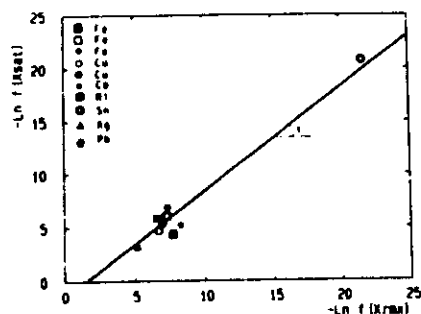


Fig. 6

Moreover, it is easy to show that eq.10-B, for small values of X_{ex} , reduces to

$$\ln \frac{X_{\text{sat}}}{X_{\text{max}}} = 3 \pm 0.5$$

11-B

Eq.11-B is very useful, because it allows the concentration corresponding to the maximum oxygen coverage to be estimated for all systems, even for those very difficult to handle from an experimental point of view, due to their very negative free energy of oxidation.

GASEOUS FLUXES AND SURFACE TENSION.

As previously shown, the surface tension of liquid metals is a quantity strongly sensitive to the degree of surface cleanliness.

In order to achieve a correct interpretation of experimental surface tension data, the exact oxygen content of the liquid phase must be known. This may be done using the Sieverts' law, which links the oxygen partial pressure in equilibrium with the liquid phase (P_2) with the oxygen molar fraction in the bulk liquid (X_2)

$$X_2 = K_2 \sqrt{P_2} \quad 12-B$$

But, the oxygen content in the liquid phase can vary with time, during an experiment, with a rate which is a function of the net flux at the liquid-vapour interface. For this reason, a description of the phenomena by using equilibrium conditions may be quite incorrect. A model has then to be applied, which allows a dynamic description of the phenomena to be made, with reference to typical experimental procedures.

Let us imagine a "sessile drop" of the liquid to be tested inside a tubular, horizontal furnace, where a flux of an inert gas (He, A) containing known amounts of oxygen (P_2), is introduced at constant temperature and flow rate.

The model is based on the following assumptions:

- The liquid surface is "plane"; this means that the drop radius, R , is large, as far as capillary effects are concerned;
- The initial oxygen content of the liquid metal is "zero";
- The gas flow rate is small (laminar flow) and maintains a constant oxygen partial pressure on a surface, placed at a distance δ from the liquid-vapour interface. This surface is considered as the origin of X coordinates;
- For each metal, M , the formation of only the more stable oxide is considered, via the reaction

$$\alpha A(g) + M(g) = MA_s(s) \quad 13-B$$

where α is the stoichiometric coefficient.

- The vapour pressure of the oxide is considered negligible;
- Total pressures P_1 are considered, which correspond to mean free paths smaller than the dimension δ . Vacuum, as a consequence, is not considered.

When the reaction 13-B can be considered irreversible, that is, when $P_2 \gg P_{2,s}$, where $P_{2,s}$ represents the partial pressure in equilibrium with the saturated solution, different kinds of reaction conditions can be defined, on the basis of the values taken by the Thiele modulus ϕ and by the parameter ϵ :

$$\phi = \delta \left(\frac{\alpha K P_{1,s}}{P_1 D_s} \right)^{1/2} \quad 14-B$$

$$\epsilon = \frac{\alpha P_{1,s} D_m}{P_1 D_s} \quad 15-B$$

where D_2 , D_m are the diffusivities of oxygen and metal vapours, $P_{2,s}$ is the vapour pressure of the liquid metal and K is the kinetic constant of reaction 13-B.

Four characteristic 'regimes' can be identified, which can describe the influence of reaction 13-B on the diffusion of the two vapour species (oxygen and metallic vapours).

Regime a: slow reactions.

In this regime, reaction 13-B has no practical effects on the diffusion. The oxygen and the metal fluxes are practically identical to those found with no reactions. This case can be formally assimilated with the case where the reaction is thermodynamically not possible.

Regime b: fast reactions with excess oxygen.

In this case, the diffusion time of the metal vapours is greater than the reaction time, with a large availability of oxygen. The reaction, which consumes all liquid metal vapours, is then confined near the liquid surface.

Regime c: fast reactions with excess metal vapours.

The oxygen diffusion times are greater than the reaction times; there is a large availability of metal vapours, so that the reaction, which consumes all oxygen atoms, is confined near $x=0$.

Regime d: instantaneous reactions.

In this domain the reaction times are much smaller than the diffusion times of both oxygen and metal vapours. The reaction is confined to a narrow, intermediate region, the "reaction surface" I , placed at $x = \delta/(1+\epsilon)$.

Fig. 7 summarizes, schematically, the conditions which can be found when a liquid metal is brought into contact with a gaseous flux containing a reactive gas. If conditions for regime a are met, irrespective of whether reaction 13-B is possible or not, a counterdiffusion of oxygen and metal vapours is set up, with oxygen adsorption rate depending mainly, on P_2/δ .

In regime b there is reaction and large availability of oxygen, which approaches the liquid surface and reacts with metal vapours.

In regime d the reaction takes place at a level I , a certain distance from the liquid surface. At this level, the equilibrium partial pressure of oxygen is reached. The flux of oxygen towards the liquid metal depends on the concentration gradient in the liquid phase, which is obviously smaller the greater the distance of I from the liquid surface.

In regime c, metal vapours are in large excess, and nearly all oxygen molecules are captured at $x \approx 0$.

In regimes c and d, the formation of a "fog" of solid oxide is possible. However, the reaction acts as a barrier for oxygen, so that the oxygen flux through the liquid-vapour interface is almost negligible.

The same treatment allows the flux at the liquid-vapour interface to be evaluated in the four different regimes. Thus, a characteristic time for the formation of a compact oxygen monolayer can be computed from the formula

$$\theta_m = M/N_{2,s} \quad 16-B$$

where M ($\approx 3 \cdot 10^{-5}$ mol/cm²) represents the number of moles in an adsorbed, compact, oxygen monolayer, and $N_{2,s}$ the oxygen flux (in mol/(cm²s)) at the liquid-vapour interface.

Table 2 shows the results of calculations for different metal-oxygen systems.

It is easily seen that, for conditions of 1 bar total pressure and 10^{-6} bar oxygen partial pressure, the times required to form a monolayer vary widely, from about half an hour to nearly the 'eternity'.

It is worth noting that this model should be perfectly valid in microgravity conditions, even better than on earth, where gases, during laminar flow, can suffer from stratification phenomena due to their different densities. Here, only the classical hypotheses of the kinetic theory of gases have been applied: it is only to be clarified if the gaseous diffusivities, which are employed to evaluate the parameters δ and ϵ may vary when passing from earth surface to a microgravitational environment.

C) SOLID-LIQUID INTERFACES.

Solid-liquid interfaces are of particular interest even in a microgravitational environment, insofar as problems related to wettability, nucleation, crystal growth phenomena and so on are concerned.

Moreover, the equilibrium shape of these interfaces are attained by means of diffusion mechanisms, so that a detailed study of the interfacial kinetics may lead to evaluate diffusion coefficients to be compared to those found on earth.

Solid-liquid interfacial tension is the most relevant parameter which can be used to describe the phenomena already mentioned: for this reason we shall present here the main techniques that can be used to measure it. In addition, an overview will be presented of the theories describing the kinetics of interfacial equilibration and of their use to evaluate the diffusion processes involved therein.

Solid-liquid dihedral angles.

Consider a binary A-B alloy in a temperature range where the solid phase coexists with the liquid one. At a constant pressure the equilibrium is monovariant, so that the temperature defines the composition of the two conjugate phases.

Interfacial properties are thus independent of the relative quantity of liquid and solid phases; it is then possible to choose a global composition of the metallic alloy which gives a small quantity of the liquid phase, interspersed between the solid grains.

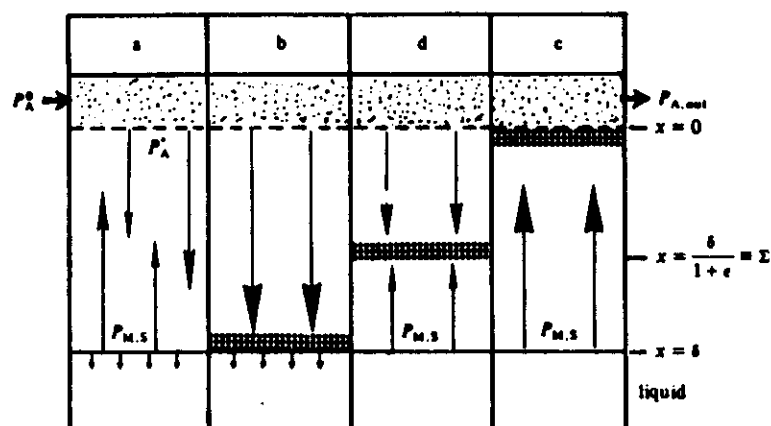


Figure 7. Representation of the physicochemical conditions in the region near the liquid-vapour interface under the four different reaction regimes.

Table 2. Calculated values for fluxes and characteristic times for metals whose surface tension has been measured as a function of their oxygen content ($P_A^0 = 10^{-6}$ bar; $P^T = 1$ bar; $fP = 0.15$).

Metal	Oxide	T/K	Reaction regime	$N_{A,S_1}/\text{mol cm}^{-2} \text{ s}^{-1}$	θ_b/s	θ_m/s
Ag	Ag ₂ O	1234	absent	9.4×10^{-13}	1.5×10^6	3.2×10^3
"	"	1734	"	6.7×10^{-13}	1.4×10^6	4.5×10^3
Al	Al ₂ O ₃	933	b	1.25×10^{-12}	3.6	2.4×10^3
"	"	1433	c	6.7×10^{-12}	4.6×10^{28}	4.4×10^{27}
Au	Au ₂ O ₃	1338	absent	8.7×10^{-13}	-	3.4×10^3
"	"	1538	"	7.6×10^{-13}	-	3.9×10^3
Co	CoO	1767	absent	6.6×10^{-13}	2.6×10^6	4.5×10^3
"	"	1967	"	5.9×10^{-13}	8.5×10^6	5.1×10^3
Cu	Cu ₂ O	1358	absent	8.6×10^{-13}	2.7×10^6	3.5×10^3
"	"	1858	"	6.3×10^{-13}	4.2×10^6	4.8×10^3
Fe	FeO	1809	c	1.02×10^{-15}	1.1×10^{11}	2.9×10^6
"	"	2009	c	2.08×10^{-16}	1.2×10^6	1.4×10^6
Ni	NiO	1728	absent	6.7×10^{-13}	5.3×10^6	4.4×10^3
"	"	1928	"	6.05×10^{-13}	1.8×10^6	4.9×10^3
Pb	PbO	601	b	1.9×10^{-12}	2.8×10^3	1.5×10^3
"	"	1101	c	2.2×10^{-10}	2.0×10^{13}	1.4×10^6
Sn	SnO ₂	505	b	2.3×10^{-12}	2.9	1.3×10^3
"	"	1005	b	1.2×10^{-12}	2.9×10^6	2.6×10^3

If the alloy is maintained for a sufficiently long time at a certain temperature in the two-phase region, the morphology of the solid-liquid interfaces will take the equilibrium shape depending on the values of the interfacial energies. In particular, the liquid phase tends to spread along the grain boundaries, and dihedral angles randomly oriented form at the junction between two solid grains. (Fig 9).

This dihedral angle has a well defined value for a certain couple of phases, is a function of temperature and depends, at equilibrium, on the relative values of solid-solid and solid-liquid interfacial tensions. It is easy to show that

$$\sigma_{gb} = 2 \sigma_{sl} \cos \phi \quad 1-C$$

where σ_{gb} represents the grain boundary tension, σ_{sl} the solid-liquid interfacial tension and 2ϕ the dihedral angle. (Fig 9)

If the solid-liquid interfacial tension is larger than the intergranular tension, 2ϕ will be greater than 120° ; on the contrary, if the intergranular tension is greater than the interfacial tension, 2ϕ will be less than 120° . When σ_{gb} is greater than two times σ_{sl} eq. 1-C is no longer valid, and the liquid phase will tend to wet completely the grain boundary. In this case the microstructure of the alloy will consist of solid grains immersed in a continuous network of the 'liquid' phase; otherwise, the liquid phase will concentrate in islands at the grain boundaries and, sometimes, even inside the grains.

The true dihedral angle can be evaluated directly in transparent systems, but, in the case of metallic alloys, a different methodology has to be applied. Harker and Parker, Smith and Riegger and Van Vlack have demonstrated that it is possible to calculate the true dihedral angle by measuring a sufficiently high number of junction angles on a random metallographic section of a polycrystalline alloy, and applying a suitable statistical treatment to the measured data.

From the distribution curve of the measured junction angles the true value of the equilibrium dihedral angle can be easily calculated as the angle corresponding to the inflection point of this curve. (Fig 10)

The behaviour of the dihedral angles as a function of temperature is different for the different systems considered, and it can be linked to the shape of the phase diagram.

In the systems presenting an eutectic point shifted towards the pure metal A (Zn-Sn, Zn-In, Al-Sn etc.) the dihedral angle decreases regularly with increasing temperature and tends to reach zero; in systems presenting a miscibility gap in the liquid phase (Zn-Pb, Zn-Bi, Al-In, Cu-Pb etc.) the dihedral angle does not vary very much in a large temperature range and then decreases sharply when reaching the monotectic temperature.

From the knowledge of the dihedral angles, only the ratio σ_{gb}/σ_{sl} can be computed; however, it has been shown that if we know at least one value of the solid-solid interfacial tension, we can evaluate the solid-liquid interfacial tension and the temperature coefficients of solid-solid and of solid-liquid interfacial tensions by the dependence of the dihedral angle from temperature. It is then in turn possible to calculate, from the

knowledge of the phase diagram, the dependence of these two interfacial tensions from the composition of the system.



Fig. 8 - Microstruttura bifasica di una lega Zn-Sn ricotta dopo attacco metallografico. $T = 288^\circ\text{C}$, $I = 300\times$.

Fig. 8 - Microstructure of a biphase Zn-Sn alloy after annealing. Etched: $T = 288^\circ\text{C}$, $I = 300\times$.

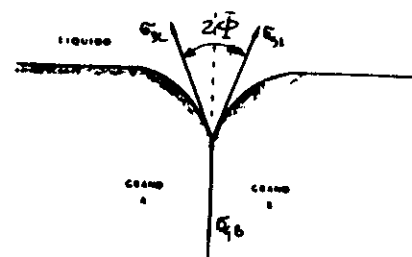


Fig. 9 - Rappresentazione schematica di una interfaccia solido-liquido.

Fig. 9 - Solid-liquid interface (schematic).

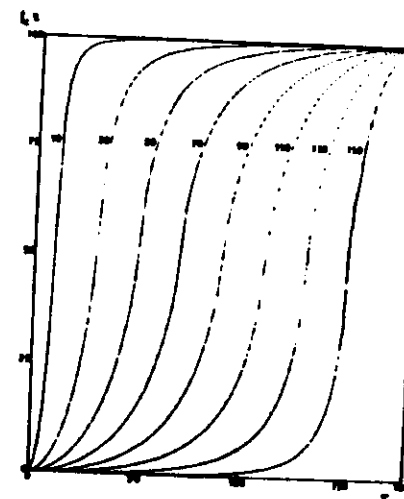


Fig. 10 - Curve di distribuzione degli angoli di giunzione per alcuni angoli diedri. Le ordinate riportano il valore della frequenza cumulativa per il valore dell'angolo di giunzione letto sulle ascisse.

